



^{68}Ga -BPAMD: PET-imaging of bone metastases with a generator based positron emitter

M. Fellner ^a, B. Biesalski ^c, N. Bausbacher ^d, V. Kubíček ^b, P. Hermann ^b, F. Rösch ^{a,*}, O. Thews ^{e,**}

^a Institute of Nuclear Chemistry, Johannes Gutenberg University of Mainz, Mainz, Germany

^b Department of Inorganic Chemistry, Charles University, Prague, Czech Republic

^c Institute of Physiology and Pathophysiology, University Medicine Mainz, Mainz, Germany

^d Department of Nuclear Medicine, University Hospital, 55101, Mainz, Germany

^e Institute of Physiology, Martin-Luther-University, Halle (Saale), Germany

ARTICLE INFO

Article history:

Received 31 October 2011

Received in revised form 10 April 2012

Accepted 21 April 2012

Keywords:

Ga-68

Macrocyclic ligand

Bisphosphonate

Bone metastases

ABSTRACT

Purpose: Bone metastases are a serious aggravation for patients suffering from cancer. Therefore, early recognition of bone metastases is of great interest for further treatment of patients. Bisphosphonates are widely used for scintigraphy of bone lesions with $^{99\text{m}}\text{Tc}$. Using the $^{68}\text{Ge}/^{68}\text{Ga}$ generator together with a macrocyclic bisphosphonate a comparable PET-tracer comes into focus.

Procedures: The bisphosphonate DOTA-conjugated ligand BPAMD was labelled with ^{68}Ga . [^{68}Ga]BPAMD was evaluated *in vitro* concerning binding to hydroxyapatite and stability. The tracer's *in vivo* accumulation was determined on healthy rats and bone metastases bearing animals by μ -PET.

Results: BPAMD was labelled efficiently with ^{68}Ga after 10 min at 100 °C. [^{68}Ga]BPAMD showed high *in vitro* stability within 3 h and high binding to hydroxyapatite. Consequently, μ -PET experiments revealed high accumulation of [^{68}Ga]BPAMD in regions of pronounced remodelling activity like bone metastases.

Conclusions: ^{68}Ga BPAMD reveals great potential for diagnosis of bone metastases via PET/CT. The straight forward ^{68}Ga -labelling could be transferred to a kit-preparation of a cyclotron-independent PET tracer instantaneously available in many clinical sites using the $^{68}\text{Ge}/^{68}\text{Ga}$ generator.

© 2012 Elsevier Inc. All rights reserved.

1. Introduction

Besides lung and liver, the bones are most frequently affected by metastases. 60%–80% of these metastases are caused by breast or prostate carcinoma. Bone metastases occur in many cases at an early stage of the tumour disease, however their symptoms are recognized rather late [1,2]. Hence, a non-invasive diagnosis of bone metastases in an early state providing a profound decision on a subsequent therapy is of great importance for patients.

$^{99\text{m}}\text{Tc}$ -phosphonates are well-established tracers for the diagnosis of bone metastases in nuclear medicine using planar imaging or single photon emission tomography (SPECT) [3]. However, due to the higher spatial resolution of positron emission tomography (PET), adequate pharmaceuticals utilizing positron emitters would be of great potential. The superior imaging quality in the case of PET/CT imaging

of bone metastases is clearly demonstrated by using [^{18}F]fluoride [4]. Moreover, PET features also quantification of the tracer accumulation in the tissues investigated, while SPECT cannot afford this. Additionally, non-cyclotron dependent PET-tracers, i.e. using radionuclide generator based nuclides, would provide the required availability for instant tracer synthesis and PET/CT diagnosis. For this attempt, the Germanium-68/Gallium-68 generator with the positron emitter ^{68}Ga ($T_{1/2} = 67.7$ min; high positron branching = 89%) represents a promising system. Having had recent supply difficulties of the $^{99}\text{Mo}/^{99\text{m}}\text{Tc}$ generators [5,6], this Gallium generator comes even more into focus of nuclear medicine diagnostics.

The cationic post-processing of the generator eluate is an excellent approach for synthesizing and evaluating new tracers [7,8]. Previous studies on first generation phosphonates [9] provided following two requirements and restrictions: Open chained ligands like EDTMP (Fig. 1) exhibit low stability with high amounts of free ligand to be injected (>1.5 mg/ kg body weight) in order to prevent complex dissociation *in vivo*. Phosphonate groups in ligands which are needed for complexing Ga^{3+} are not available for binding to apatite (e.g. NOTP; Fig. 1), thus “free” phosphonates are necessary [9].

Bisphosphonates are known to show high and fast binding to apatite structures especially those of high biological activity [10] and

* Correspondence to: F. Rösch, Johannes Gutenberg University, Institute of Nuclear Chemistry, Fritz-Strassmann-Weg 2, D-55128 Mainz, Germany.

** Correspondence to: O. Thews, Martin-Luther-University of Halle, Institute of Physiology, Magdeburger Str. 6, 06097 Halle (Saale), Germany.

E-mail addresses: frank.roesch@uni-mainz.de (F. Rösch), oliver.thews@medizin.uni-halle.de (O. Thews).

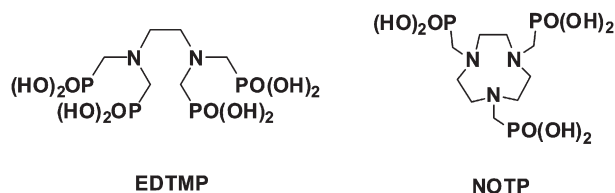


Fig. 1. Ligands EDTMP and NOTP used in former study investigating ^{68}Ga -complex formation and binding to hydroxyapatite [9].

are well-established ligands for $^{99\text{m}}\text{Tc}$ -labelled SPECT tracers. Commonly used phosphonates for $^{99\text{m}}\text{Tc}$ are bisphosphonates like methylene diphosphonate (MDP), dicarboxypropane diphosphonate (DPD) and hydroxymethylene diphosphonate (HDP). Chemically combining bisphosphonates with a positron emitter, consequently, would be of great potential for the *in vivo* imaging of bone metastases using PET/CT, particularly in times of global ^{99}Mo shortage as seen over the last years.

Combining essentials of bisphosphonate structures as targeting moieties and macrocyclic chelators for improved ^{68}Ga complex stability *in vivo* led to a new generation of DOTA bisphosphonates. One of these is (4-[[bis-(phosphonomethyl)) carbamoyl]methyl]-7,10-bis(carboxymethyl)-1,4,7,10-tetraazacyclododec-1-yl)acetic acid (BPAMD; Fig. 2) [11,12], which was labelled with ^{68}Ga in nmol scale in water after 10 min heating at 100 °C and has been used for a first human application [13].

Bisphosphonates in general are of another benefit. Compounds like alendronate, risedronate or zoledronate do not only bind to the hydroxyapatite structure of the bone, they are also interacting in the HMG CoA reductase pathway and are inhibiting the farnesyl diphosphate synthase (FPPS) [10,14]. The bisphosphonates mimic pyrophosphates and thus inhibit the FPPS meaning that bisphosphonates express biochemical targeting and not only a physico-chemical binding to hydroxyapatite structures of the bone matrix.

2. Materials and methods

2.1. Generator

Germanium-68 ($T_{1/2} = 270.8$ days) provides the positron emitter Gallium-68 as an easily available and relatively inexpensive source of a PET nuclide. A Cyclotron Obninsk Ltd. Co. (Russian Federation) generator was used, with Germanium-68 fixed on a solid phase of modified titanium dioxide. Gallium-68 is eluted from the generator with 10 mL 0.1 M HCl and is online-immobilized on a strong acidic cation exchanger. A 1 mL mixture of hydrochloric acid and acetone further removes impurities such as zinc, iron and titanium as well as ^{68}Ge generator breakthrough (0.15 M HCl/80% acetone). Subsequently, ^{68}Ga is eluted quantitatively in 400 μL of a second mixture of HCl and acetone (0.05 M HCl/97.6% acetone) from the cation exchange resin [7,8]. This fraction serves as an ideal low-

volume, low acidic and chemically highly pure source of ^{68}Ga for subsequent labelling.

2.2. BPAMD synthesis and labelling

BPAMD was prepared by published method [11,12]. In brief, triethyl orthoformate (1.2 eq.), diethyl phosphite (3 eq.), and dibenzylamine (1 eq.) were reacted at 150 °C for 5 h with condenser and additional 24 h without. The reaction mixture was partitioned between CHCl_3 and 5% aqueous NaOH and washed with brine. The crude product was purified by gradient column chromatography over ethanol/ hexane yielding tetraethyl (*N,N*-dibenzyl)aminomethyl-bis(phosphonate) (43%). This compound was hydrogenated using 10% Pd/C in ethanol, yielding tetraethyl aminomethyl-bis(phosphonate) in 96% yield as colourless oil. This product was dropped in a solution of chloroacetyl chloride in acetonitrile, cooled to -40 °C. Treated with charcoal and removing excess of chloroacetyl chloride by co-distillation with toluene gave the chloroacetamide as colourless oil (96%). Finally the chloroacetamide was dissolved in acetonitrile together with K_2CO_3 and added to a solution of $t\text{-Bu}_3\text{DO}_3\text{A}\cdot\text{HBr}$ in acetonitrile with K_2CO_3 . Reaction overnight, subsequent evaporation of the solvent and deprotection of the tert-butyl ester yielded the product BPAMD after purification over a strong cation exchanger (39%).

A stock solution of BPAMD (1 mg/mL water) was prepared and aliquots were used for labelling studies. ^{68}Ga labelling itself was performed in 5 mL Millipore water in 11 mL Technivials by adding 400 μL of purified and concentrated ^{68}Ga fraction. Through variation of reaction time (1–10 min), temperature (60 to 100 °C), different amounts of the complex ligands (5–50 nmol) as well as reaction pH (pH = 1–5), optimum reaction parameters for ^{68}Ga complex formation were analysed. All experiments studying labelling kinetics were conducted in a Thermomixer system (HLC Biotech Heating Thermo-Mixer MHR 13). For human application, the Thermomixer can be replaced by a simple heating block available at most clinical sites with a $^{68}\text{Ge}/^{68}\text{Ga}$ generator.

2.3. Radioactive analysis

Determinations of radiochemical labelling yield and complex formation kinetics were carried out by two TLC systems: A: Merck SG-60 silica plates developed with 0.25 M citrate buffer pH 4; B: Macherey Nagel cellulose TLC plates (Polygram Cel 300, 0.1 mm) developed with 2:1 mixture of B1:B2 (B1: 9 mL Millipore water; 0.6 mL HCl (conc. 37%); 88 mL acetone/B2: 2,4-pentadione). After drying and developing, TLCs were measured on a Canberra Packard Instant Imager.

Additionally an HPLC system was developed for quality control using a strong anion exchange column (Partisil 10 SAX 250×4 mm) on a Dionex HPLC system (P680 HPLC, UVD 170U) connected with a Raytest Gabi 2×2 " radioactivity detector. The solvent system was a gradient of 1 M phosphate buffer (pH = 3, A) and 1 M sodium citrate (B): flow 1.5 mL/min; 0–5 min 100% A; 5–7 min 100% A to 70% A/30% B; 7–12 min 70% A/30% B; 12–14 min 70% A/30% B to 100% A; 14–20 min 100% A.

2.4. Purification of [^{68}Ga]BPAMD

Non-complexed ^{68}Ga had to be removed prior to further evaluations. This was performed by passing the reaction mixture over strong cation exchanger (Strata-X-C 60 mg, conditioned with 1 mL 4 M HCl and 1 mL water). The non-complexed gallium was immobilized on the exchanger while the [^{68}Ga]BPAMD complex passed to the product vial. In order to adjust the pH to 7.4, aliquots of a 100 mg/mL sodium HEPES solution were added.

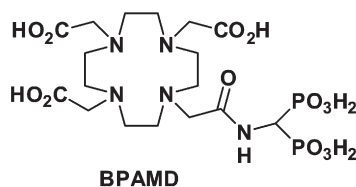


Fig. 2. Bisphosphonate ligand BPAMD investigated in this study.

2.5. Binding studies on hydroxyapatite

Binding studies on synthetic hydroxyapatite (Hap, Sigma-Aldrich) were applied to *in vitro* simulate the binding of the ^{68}Ga ligand complex to bone structures. For this purpose, 20 mg Hap was incubated in 1 mL isotonic saline for 24 h. The test itself was performed by the addition of 50 μL (about 3 nmol of complex and inactive ligand all together) of the ^{68}Ga -complexes to the Hap fraction. After vortexing for 10 s, the probes were incubated for 10 min at ambient temperature. The samples were centrifuged and the supernatant was removed. The Hap fraction was washed with 0.5 mL saline. This solution contained less than 2% of the overall ^{68}Ga radioactivity.

The ^{68}Ga radioactivity in combined liquids and the Hap fraction was measured in a curiemeter (Aktivimeter Isomed 2010, MED Nuklear-Medizintechnik Dresden GmbH). ^{68}Ga complex binding to Hap was determined as per cent of ^{68}Ga absorbed to Hap.

2.6. Stability study in vitro

For stability study, 3 mg of apo-transferrin (Sigma-Aldrich) was suspended in 1 mL PBS buffer (Sigma-Aldrich). 400 μL of purified ^{68}Ga]BPAMD was added. The mixture was shaken in the Thermomixer at 37 °C for up to 180 min. The solution was analysed by TLC using 0.25 M citrate buffer pH 4. For control, additional vials were prepared by the same method only missing one compartment (chelator or transferrin) and therefore serving as complete binding of ^{68}Ga to transferrin (without chelator) and only ^{68}Ga]BPAMD (without transferrin).

2.7. Animals and tumours

Animal imaging experiments were performed both in healthy rats (Copenhagen rat, body weight 190 g) and in animals bearing induced bone metastases (Sprague–Dawley rats). Animals were allowed access to food and acidified water *ad libitum* before the investigation. All experiments had previously been approved by the regional animal ethics committee and were conducted in accordance with the German Law for Animal Protection and the UKCCCR Guidelines [15].

For metastases experiments, cells of the Walker 256 mammary carcinoma of the rat have been used, a cell line which is known to form bone metastases [16]. Walker 256 cells were obtained from ATCC (LGC Standards GmbH, Wesel, Germany) and grown in RPMI medium supplemented with 10% fetal calf serum (FCS) at 37 °C under a humidified 5% CO_2 atmosphere and sub-cultivated once per week. For tumour implantation male Sprague–Dawley rats (Charles River Wiga,

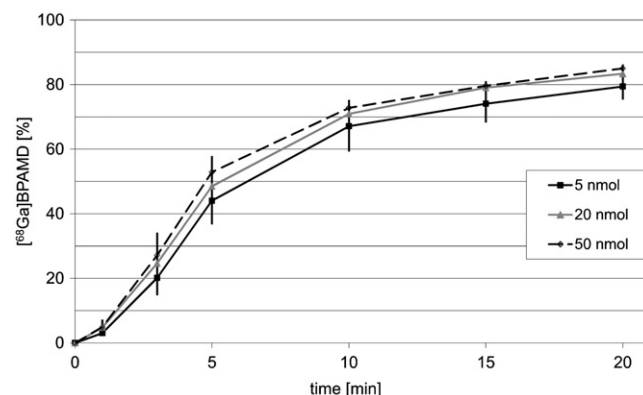


Fig. 4. Radiochemical yield of ^{68}Ga]BPAMD at 100 °C and pH=3 with different amounts of ligand (5–50 nmol, n=4, TLC-system A for analysis, cross checked with system B).

Sulzfeld, Germany; body weight 320 to 480 g) housed in the animal care facility of the University of Mainz were used in this study. For metastasis induction Walker 256 cells were injected into the superficial caudal epigastric artery [17]. In brief, after an inguinal incision the subcutaneous preparation of the epigastric artery was performed. After distal ligation of the artery a thread was looped loosely around the proximal end. Following a small incision of the artery wall a catheter (o.d. 0.5 mm, i.d. 0.25 mm) was inserted and fixed with the thread. 2×10^5 cells were suspended in 200 μL isotonic saline and injected into the catheter. After tightening the proximal ligature the catheter was removed, the operating field was cleaned with ethanol and the cutaneous incision was closed. Tumour cells were always implanted into the left leg whereas the contralateral side served as a control. Previous experiments showed that with this procedure bone metastases in the distal femur or the tibia were formed in approximately 80% of the animals 2 weeks after tumour cell injection [17]. For this reason μ -PET imaging was performed after 14 days.

2.8. μ -PET experiments

PET imaging was performed in spontaneously breathing rats under isoflurane anaesthesia (2% isoflurane, 98% oxygen). ^{68}Ga]BPAMD was prepared with 30 nmol ligand using the described conditions. After purification and pH adjustment, a solution was obtained ready for injection.

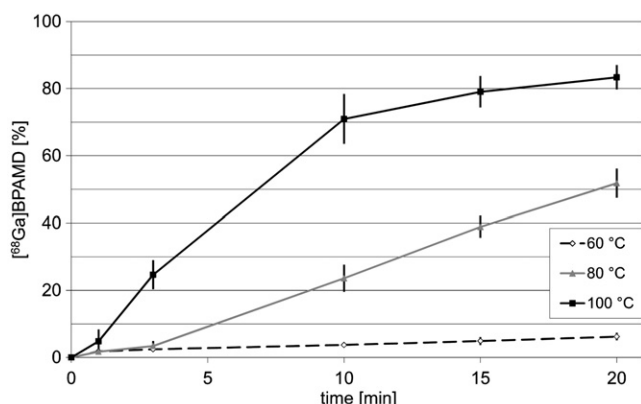


Fig. 3. Radiochemical yield of ^{68}Ga]BPAMD at different temperatures with 20 nmol BPAMD at pH=3 (n=4, TLC-system A for analysis, cross checked with system B).

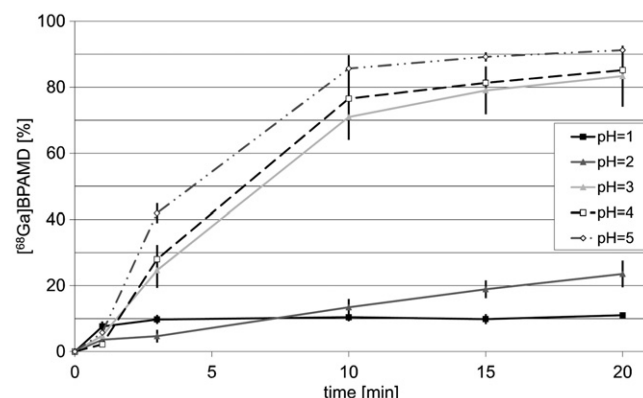


Fig. 5. Radiochemical yield of ^{68}Ga]BPAMD using 20 nmol ligand at 100 °C with pH varied from 1 to 5 (n=4, TLC-system A for analysis).

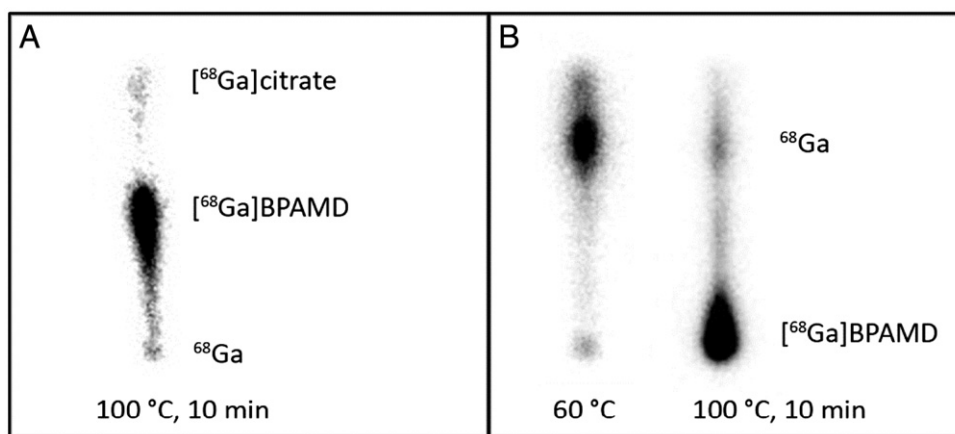


Fig. 6. A) Citrate TLC of the reaction mixture of [^{68}Ga]BPAMD, $R_f=0.0$: ^{68}Ga , $R_f=0.5$: [^{68}Ga]BPAMD, $R_f=0.9$: ^{68}Ga -citrate; B) cellulose TLC with solvent system B1:B2 (2:1) with $R_f=0.0$: [^{68}Ga]BPAMD, $R_f=0.8$: ^{68}Ga .

The μ -PET imaging was performed on a microPET Focus 120 small animal PET (Siemens/Concorde, Knoxville, USA). During PET measurements the animals were placed in supine position. For imaging of the healthy animals the scanning region was placed over the chest whereas in the tumour experiments the region was located over the lower limb from the pelvis down to the feet. After a 15 min transmission scan with an external ^{57}Co source, dynamic PET studies were acquired in 2D mode. The radiotracer was administered as a bolus injection via the tail vein. For the measurement of the tracer distribution in a healthy animal the injected dose was 15 MBq. In the metastases experiments the dose was 20.5 ± 0.5 MBq. Afterwards, PET images were obtained for a total measuring interval of 60 min. Finally, a whole body scan (60–75 min post injection) was performed.

For analysis the PET listmode data were histogrammed into 14 to 20 frames with varying time frames (1–5 min) and reconstructed using OSEM algorithm. μ -PET image quantification was applied using PMOD software (PMOD Technologies Ltd.). Volumes-of-interest (VOIs) were defined for tumour and reference tissue (contralateral bone). Ratios of tumour to reference tissue were calculated from integral image between 10' and 60' after tracer injection.

3. Results

3.1. Complex formation, analysis and purification

The elution of $^{68}\text{Ga}^{3+}$ from the generator and the on line-processing of the eluate are performed within less than five minutes. Figs. 3 to 5 compare typical labelling reactions for BPAMD depending on temperature (Fig. 3, 60 to 100 °C), amount of ligand (Fig. 4, 5–50 nmol) and reaction pH (Fig. 5, pH = 1–5).

Labelling finally proceeds at temperatures of 100 °C within 10 min in a total volume of 5 mL and at optimal pH of 3 to yield 90% of [^{68}Ga]BPAMD. This was checked by TLC and HPLC: TLC with sodium citrate showed the complex with an $R_f=0.5$ and uncomplexed ^{68}Ga with $R_f=0.0$ and 0.9 (due to formation of ^{68}Ga -citrate with solvent front and possibly colloidal ^{68}Ga at the origin) whereas the second solvent system showed 2 spots only and takes only 5 min for developing, compared to about 15 min for the citrate TLC. The complex [^{68}Ga]BPAMD is identified at $R_f=0.0$ and uncomplexed ^{68}Ga at $R_f=0.8$ (Fig. 6).

HPLC revealed two peaks, the complex [^{68}Ga]BPAMD at 3.2 min and the uncomplexed ^{68}Ga at 8.5 min (Fig. 7). Both analytical methods were found to be consistent among the analysis methods (90% by TLC compared to 91% by HPLC).

The reaction mixture was purified from uncomplexed ^{68}Ga using 60 mg Strata-X-C columns yielding pure [^{68}Ga]BPAMD (>98% radiochemical purity by HPLC, Fig. 8). Prior to using the purified [^{68}Ga]BPAMD for binding and μ -PET studies, pH was adjusted to 7.4 by adding aliquots of a sodium HEPES solution.

3.2. Hydroxyapatite binding

Hydroxyapatite experiments showed binding of $81.5 \pm 0.5\%$ for [^{68}Ga]BPAMD. Compared to former studies under the same conditions with the NOTA tri-phosphonate (NOTP) and an open chained phosphonate (EDTMP) the binding is lower than for [^{68}Ga]EDTMP (Fig. 9). However, in previous studies EDTMP showed a very low *in vivo* stability [9] with a rapid decomposition of the complex. For this reason [^{68}Ga]BPAMD is more favourable for *in vivo* experiments in animals.

3.4. Stability study

Stability study of [^{68}Ga]BPAMD against 3 mg apo-transferrin revealed a decomposition of $9.1 \pm 0.6\%$ ($n=5$) within 3 h at 37 °C. However, this decomposition was also present in PBS buffer under the same experimental conditions but with a lower value of $4.2 \pm 0.8\%$ ($n=5$). Due to the very limited *in vivo* stability of [^{68}Ga]EDTMP [9] a comparative determination of the biodistribution of BPAMD and EDTMP was not possible. However, with 50 nmol ^{68}Ga EDTMP imaging showed only negligible uptake at the skeleton indicating a lower *in vivo* specificity of EDTMP as compared with BPAMD.

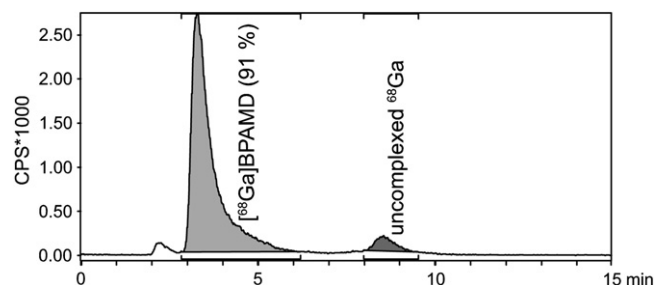


Fig. 7. HPLC radioactivity chromatogram of the reaction mixture of [^{68}Ga]BPAMD (20 nmol BPAMD, 100 °C, 10 min); retention times: [^{68}Ga]BPAMD at 3.2 min, uncomplexed ^{68}Ga at 8.5 min.

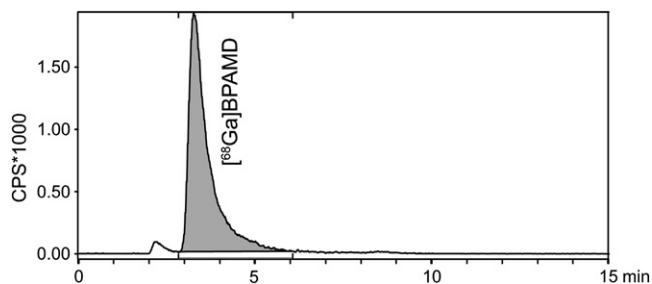


Fig. 8. HPLC radioactivity chromatogram of purified $[^{68}\text{Ga}]$ BPAMD, radiochemical purity >98%.

3.5. μ -PET small animal study

Imaging the $[^{68}\text{Ga}]$ BPAMD uptake in a healthy animal showed that the tracer is accumulated in bones most prominent in sections with a relatively high turnover of the bone matrix. Under physiological conditions rats show high remodelling activity in the joints. For this reason the $[^{68}\text{Ga}]$ BPAMD accumulation was highest in the shoulder and along the backbone (Fig. 10). Compared to solid bones, the accumulation in the joints of the vertebral column was higher by a factor of 2.49 (humerus), 2.88 (sternum) or 2.08 (scapula). These data indicate that the new tracer preferentially accumulates in metabolically active bone regions.

For the metastasis experiments, Walker 256 cells were injected into the superficial caudal epigastric artery of the right leg of 7 animals. Within 2 weeks five of them developed a bone metastasis in the tibia (confirmed by histology after PET imaging) whereas 2 animals did not show any signs of tumour growth. All metastases were located in the proximal end or the shaft of the tibia [17]. Using $[^{68}\text{Ga}]$ BPAMD for PET imaging the tracer was accumulated within the metastases (Fig. 11). Compared to the contralateral tibia (which served as an intraindividual control), the accumulation in the metastatic lesion was 3.97 ± 1.82 times higher ($n = 4$).

4. Discussion

4.1. ^{68}Ga -complex formation, analysis and purification

Complex formation of $[^{68}\text{Ga}]$ BPAMD is fast and results in high yields. However, it was not possible to gain the tracer in quantitative yield. Around 90% seems to be the maximum yield for 10 min reaction time with heating to 100 °C. Nevertheless subsequent cartridge-based purification is fast and efficient. $[^{68}\text{Ga}]$ BPAMD can be obtained in 20–25 min starting from elution of the generator in 62% decay corrected yield, ready for further application. As important the fast and easy labelling procedure for a clinical adoption is, also the fast analysis and quality control of the final product are of great significance. The presented TLC and HPLC systems provide analytical

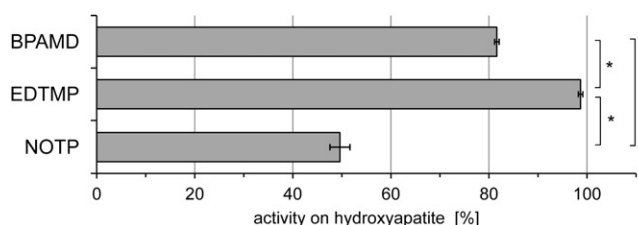


Fig. 9. *In vitro* binding of ^{68}Ga complexes (only ligands are given) to hydroxyapatite; comparison of BPAMD to ligands used in previous study (EDTMP, NOTP) [9]. $n = 4$, (*) $p < 0.05$.

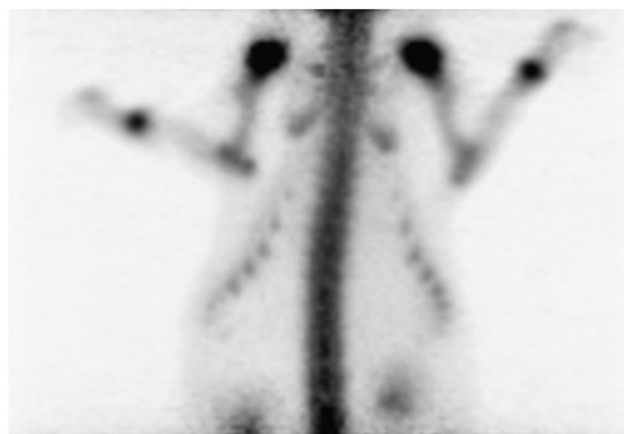


Fig. 10. Example of 15 MBq of $[^{68}\text{Ga}]$ BPAMD accumulation in bones of healthy rat under isoflurane anaesthesia as MIP from an integral image 15–60 min p.i.

results ready in less than 10 min which is of great advantage in the context of human application.

4.2. Hydroxyapatite binding

Binding experiments with hydroxyapatite show a trend for the *in vitro* binding of various phosphonates. The literature describes many different experimental setups [18–20]. Although the model is simplifying specific binding characteristics it seems to be possible to distinguish between compounds applicable for further studies for example in animals and those that will not be evaluated further. It does not, for example, show any biological activity of the tracer, as it is proposed for the bisphosphonates, inhibiting the FPP synthase [10,14].

4.3. Stability study

Investigation of the complex stability at 37 °C showed only small decrease over a time of 3 h in PBS buffer and against apo-transferrin, however, to an insignificant extent (4.2% in PBS; 9.1% against apo-transferrin). This decomposition of $[^{68}\text{Ga}]$ BPAMD is of minor impact since the released ^{68}Ga will be rapidly bound to transferrin *in vivo* [21]. Since $[^{68}\text{Ga}]$ -transferrin will be eliminated from the blood compartment by more than 70% within 60 min [21,22] the decomposition measured *in vitro* after 3 h will only marginally affect the accumulation of $[^{68}\text{Ga}]$ BPAMD. However, since free ^{68}Ga can also be bound to other circulating anions the disaggregation might result in a slight fall of image contrast.

4.4. μ -PET small animal study

In the animal experiments it was shown that the new tracer basing on the macrocyclic bisphosphonate BPAMD labelled with ^{68}Ga is taken up into the bone especially in regions with a high remodelling activity. In particular in the epiphysis of the bones close to joints and in the backbone, activity higher uptake of the tracer was found. These regions could be visualized with a high spatial resolution (Fig. 10).

The animal model used for induction of bone metastases by injecting tumour cells into the superficial caudal epigastric artery (a branch of the femoral artery) is known to lead to orthotopic metastases [23]. Using the cell line Walker 256, metastases were induced in the present experiments in 70% of the animals, a rate, which is comparable to previous results with the same model. In the previous experiments approximately 80% of the animals had osteolytic lesions, which were located mostly in the proximal shaft

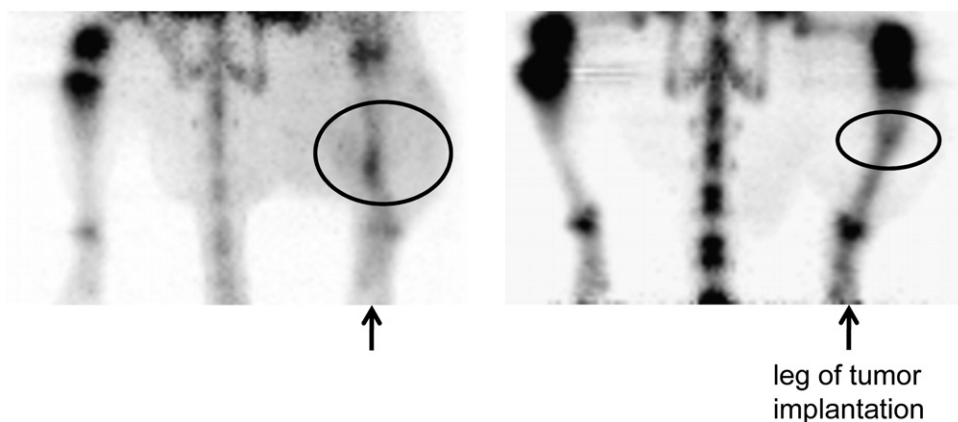


Fig. 11. Two examples of *in vivo* accumulation of 20.5 ± 0.5 MBq [^{68}Ga]BPAMD in bone metastases (circles of two animals). Tumour cells were injected into the superficial caudal epigastric artery of the right leg. PET imaging was performed two weeks after tumour implantation. Animals were investigated under isoflurane anaesthesia. Images show MIP from integral images 15–60 min p.i.

or the head of the tibia [17]. For this reason, the animal model used is a realistic representation of bone metastases of breast or prostate cancers. It is important to point out that at the site of the bone tumour no additional injury was made leading to a forced remodelling in the bone. Activity changes in the bone were solely by the incorporation of the tumour cells.

In these experimental metastases [^{68}Ga]BPAMD showed a significant accumulation (Fig. 11). In all animals exhibiting tumours in the leg, the lesions were clearly identifiable in the PET images. The relative activity of the tracer was approximately 4-times higher than in the contralateral leg without a tumour. The imaging allowed to identify metastases with a diameter of 1–3 mm. These results clearly indicate that [^{68}Ga]BPAMD is suitable as a tracer for bone metastases in PET imaging.

Interestingly, the ratio between bone and soft tissue accumulation was high (contrast factor ~ 15) and allowed excellent visualisation of small bone metastases, already observed for a first human study. In addition, significant uptake ratios for bone metastases and normal bone are achieved, fulfilling another important criterion for useful imaging tracers. This result exactly confirms our expectation concerning improved complex stability and imaging quality already at lowest complex ligand concentration (~ 5 nmol per animal).

5. Conclusion

Investigation of labelling kinetics of BPAMD with ^{68}Ga showed best efficiency at pH = 3–5 and 100°C for 10 min with a radiochemical yield of 90%. As quantitative yield could not be achieved, efficient purification from uncomplexed ^{68}Ga was applied using strong cation exchanger columns. For quality control TLC and HPLC systems were developed, showing the high purity ($>98\%$) of the product [^{68}Ga]BPAMD in less than 10 min. Studies of hydroxyapatite revealed 81.5% binding of the tracer to the synthetic bone material. Decomposition of [^{68}Ga]BPAMD when challenged with apo-transferrin was very small (9.1% after 3 h), leading to first *in vivo* experiments on a healthy rat with μ -PET. Images showed high accumulation on joints, implying high remodelling activity of these bone structures in rats. Consequently in further experiments Walker 256 carcinoma cells were injected on the right leg of rats, developing osteolytic lesions, located mostly in the proximal shaft or the head of the tibia. Injection of [^{68}Ga]BPAMD and μ -PET imaging focused on the legs of the animals indicated high contrast between the bone lesion and healthy bone in the same animal (contrast factor = 3.97 ± 1.82).

Altogether, [^{68}Ga]BPAMD is of great interest for nuclear medicine. By using the $^{68}\text{Ge}/^{68}\text{Ga}$ generator the tracer can be obtained in a fast and easy process within 20–25 min ready for injection.

Having the higher spatial resolution as well as quantification PET-technique is superior to SPECT with $^{99\text{m}}\text{Tc}$ -phosphonates and it is cyclotron independent.

6. Conflict of Interest

The authors declare that they have no conflict of interest.

Acknowledgment

Cooperation within COST D38 and COST BM0607 is gratefully acknowledged. The study was supported by Deutsche Krebshilfe (grant 109136).

References

- [1] Greenlee RT, Hill-Harmon MB, Murray T, Thun M. Cancer statistics, 2001. *CA Cancer J Clin* 2001;51:15–36.
- [2] Rubens RD. Bone metastases—the clinical problem. *Eur J Cancer* 1998;34:210–3.
- [3] Zetting G, Leitha T, Niederle B, Kaserer K, Becherer A, Kletter K, et al. FDG positron emission tomographic, radioiodine, and MIBI imaging in a patient with poorly differentiated insular thyroid carcinoma. *Clin Nucl Med* 2001;26:599–601.
- [4] Harmer CL, Burns JE, Sams A, Spittle M. The value of fluorine-18 for scanning bone tumours. *Clin Radiol* 1969;20:204–12.
- [5] Ballinger JR. ^{99}Mo shortage in nuclear medicine: crisis or challenge? *J Label Compd Radiopharm* 2012;53:167–8.
- [6] Gould P. Medical isotope shortage reaches crisis level. *Nature* 2009;460:312–3.
- [7] Asti M, De PG, Fraternali A, Grassi E, Sghedoni R, Fioroni F, et al. Validation of $^{68}\text{Ge}/^{68}\text{Ga}$ generator processing by chemical purification for routine clinical application of ^{68}Ga -DOTATOC. *Nucl Med Biol* 2008;35:721–4.
- [8] Zhernosekov KP, Filosofov DV, Baum RP, Aschoff P, Bihl H, Razbash AA, et al. Processing of generator-produced ^{68}Ga for medical application. *J Nucl Med* 2007;48:1741–8.
- [9] Fellner M, Riss P, Loktionova N, Zhernosekov KP, Thews O, Gerales CFGC, et al. Comparison of different phosphorus-containing ligands complexing ^{68}Ga for PET-imaging of bone metabolism. *Radiochim Acta* 2011;99:43–51.
- [10] Papapoulos SE. Bisphosphonates: how do they work? *Best Pract Res Clin Endocrinol Metab* 2008;22:831–47.
- [11] Kubicek V, Rudovský J, Kotek J, Hermann P, Vander Elst L, Muller RN, et al. A bisphosphonate monoamide analogue of DOTA: a potential agent for bone targeting. *J Am Chem Soc* 2005;127:16477–85.
- [12] Vitha T, Kubicek V, Hermann P, Vander Elst L, Muller RN, Kolar ZI, et al. Lanthanide(III) complexes of bis(phosphonate) monoamide analogues of DOTA: bone-seeking agents for imaging and therapy. *J Med Chem* 2008;51:677–83.
- [13] Fellner M, Baum RP, Kubicek V, Hermann P, Lukeš I, Prasad V, et al. PET/CT imaging of osteoblastic bone metastases with ^{68}Ga -bisphosphonates: first human study. *Eur J Nucl Med Mol Imaging* 2010;37:834.
- [14] Ebetino FH, Rozé ZN, McKenna CE, Barnett BL, Dunford JE, Russell RGG, et al. Molecular interactions of nitrogen-containing bisphosphonates within farnesyl diphosphate synthase. *J Organomet Chem* 2005;690:2679–87.
- [15] Workman P, Twentyman P, Balkwill F, Balmain A, Chaplin DJ, Double JA, et al. United Kingdom Co-ordinating Committee on Cancer Research (UKCCCR) guidelines for the welfare of animals in experimental neoplasia (2nd edit.). *Br J Cancer* 1998;77:1–10.

- [16] Kostenuik PJ, Singh G, Suyama KL, Orr FW. A quantitative model for spontaneous bone metastasis: evidence for a mitogenic effect of bone on Walker 256 cancer cells. *Clin Exp Metastasis* 1992;10:403–10.
- [17] Biesalski B, Yilmaz B, Buchholz HG, Bausbacher N, Schreckenberger M, Thews O. An allogenic site-specific rat model of bone metastases for nuclear medicine and experimental oncology. *Nucl Med Biol* 2011;39:502–6.
- [18] Försterová M, Jandurová Z, Marques F, Gano L, et al. Chemical and biological evaluation of ^{153}Sm and ^{166}Ho complexes of 1,4,7,10-tetraazacyclododecane-1,4,7,10-tetrakis(methylphosphonic acid monoethylester) ($\text{H}_4\text{dotp}^{\text{OEt}}$). *J Inorgan Biochem* 2008;102:1531–40.
- [19] Mitterhauser M, Toegel S, Wadsak W, Lanzenberger RR, Mien IK, Kuntner C, et al. Pre vivo, ex vivo and in vivo evaluations of ^{68}Ga -EDTMP. *Nucl Med Biol* 2007;34:391–7.
- [20] Okamoto Y. Accumulation of technetium-99m methylene diphosphonate. Conditions affecting adsorption to hydroxyapatite. *Oral Surg Oral Med Oral Pathol Oral Radiol Endod* 1995;80:115–9.
- [21] Brunetti A, Blasberg RG, Finn RD, Larson SM. Gallium-transferrin as a macromolecular tracer of vascular permeability. *Int J Rad Appl Instrum B* 1988;15:665–72.
- [22] Ferreira CL, Lamsa E, Woods M, Duan Y, Fernando P, Bensimon C, et al. Evaluation of bifunctional chelates for the development of gallium-based radiopharmaceuticals. *Bioconj Chem* 2010;21:531–6.
- [23] Bäuerle T, Adwan H, Kiessling F, Hilbig H, Armbruster FP, Berger MR. Characterization of a rat model with site-specific bone metastasis induced by MDA-MB-231 breast cancer cells and its application to the effects of an antibody against bone sialoprotein. *Int J Cancer* 2005;115:177–86.